# Superconductivity induced by the intervalley Coulomb scattering in a few layers of graphene

Tommaso Cea

*Department of Physical and Chemical Sciences, Universitá degli Studi dell'Aquila, I-67100 L'Aquila, Italy*

We study the intervalley scattering induced by the Coulomb repulsion as a purely electronic mechanism for the origin of superconductivity in a few layers of graphene. The pairing is strongly favored by the presence of van Hove singularities in the density of states. We consider three different heterostructures: twisted bilayer graphene, rhombohedral trilayer graphene, and Bernal bilayer graphene. We obtain trends and estimates of the superconducting critical temperature in agreement with the experimental findings, which might identify the intervalley Coulomb scattering as a universal pairing mechanism in a few layers of graphene.

## I. INTRODUCTION

The discovery of superconductivity (SC) in twisted bilayer graphene (TBG) [1–3] led the scientific community to a renewed interest in the study of the SC properties of graphene, that has been further motivated by the more recent observations of SC behavior in other heterostructures based on graphene: twisted trilayer graphene (TTG) [4], untwisted rhombohedral trilayer graphene (RTG) [5], and Bernal bilayer graphene (BBG) [6] in a perpendicular electric field. In all these systems the SC transition can be controlled by experimentally tunable parameters, such as, e.g., the relative twist between the layers, the electronic density, and the applied displacement field. Even though the critical temperatures $T_c$ observed so far in these materials do not exceed the scale of a few degrees Kelvin, the large ratios between $T_c$ and the Fermi energy, up to ∼10%, suggest that a strong pairing interaction is at play. On the other hand, the complex phase diagrams reported in the literature clearly highlight the strongly correlated behavior. The recent observation of Ref. [7], that the value of $T_c$ in BBG can be increased by one order of magnitude by a substrate of WSe$_2$, emphasizes the highly tunable nature of the pairing, paving the way towards engineering new techniques for controlling the magnitude of $T_c$. Furthermore, the violation of the Pauli limit reported in the experiments [4–6] suggests that spin-triplet Cooper pairs are favored in these systems.

On the theoretical side, it is universally accepted that the band flattening and the vicinity of the van Hove singularities (VHSs) to the Fermi level enhance the role of the electronic interactions in TBG, TTG, RTG, and BBG, favoring the formation of symmetry broken phases (see, e.g., Refs. [8–13]). However, the debate on the mechanism at the origin of the superconductivity in these systems is still open. Many models have been studied so far, those either consider the superconductivity driven by purely electronic interactions [9,12,14–32] or by more conventional phononic mechanisms [33–43]. The combined effects of the screened Coulomb interaction, the electronic umklapp processes, and the electron-phonon coupling have been shown to favor the pairing in TBG [44–46] and in TTG [47]. Furthermore, Refs. [48–52] explored other unconventional mechanisms, in which the pairing is mediated by soft electronic collective modes. Remarkably, there is not yet a general agreement on whether the superconductivity observed in TBG and in TTG has the same origin as in the untwisted RTG and BBG.

In this Letter, we study the intervalley scattering induced by the Coulomb interaction as a purely electronic mechanism for the origin of superconductivity in a few layers of graphene. The resulting Cooper pairs are spin triplets with the two electrons in opposite valleys, $K$, $K'$, featuring $p$- or $f$-wave symmetry. Because the large momentum transfer, $\Delta K \equiv K - K'$, involved in the process makes the interaction strength negligible, a high density of states (DOS) is necessary to boost the pairing. This condition is often realized in a few layers of graphene, where the electronic bands can be flattened by tuning a number of experimental parameters, thus giving rise to VHSs. At first approximation, we neglect the contribution of the intravalley Coulomb repulsion, which is long ranged, since it is drastically screened in the van Hove scenario. We show quantitatively that this assumption is fully justified in the Supplemental Material (SM) [53]. Using effective continuum models with realistic parameters, we characterize the SC transition induced by the intervalley Coulomb scattering in TBG, RTG, and BBG, upon varying the relative twist between the layers and/or the electronic density and/or the displacement field. We obtain estimates and trends of $T_c$ in good agreement with the experimental results, emphasizing the strong enhancement of $T_c$ by the presence of VHSs. Remarkably, our calculations account for the different orders of magnitude of the critical temperatures observed in different materials. Considering also the experimental evidence of spin-triplet superconductivity in these systems, our study might identify the intervalley Coulomb scattering as a universal driving mechanism for the superconductivity observed so far in a few layers of graphene. We also identify a nontrivial structure of the SC order parameter (OP) in real space.

## II. THE MODEL: EFFECTIVE ATTRACTION FROM THE INTERVALLEY SCATTERING

Our theoretical description of the pairing interaction starts from considering the Coulomb repulsion between the $p_z$

electrons within the minimal lattice model for a multilayer of graphene,

$$\hat{H}_{\text{int}} = \frac{1}{2} \sum_{\boldsymbol{R}\boldsymbol{R}'} \sum_{ij\sigma\sigma'} c_{i\sigma}^{\dagger}(\boldsymbol{R}) c_{j\sigma'}^{\dagger}(\boldsymbol{R}') V_C^{ij}(\boldsymbol{R}-\boldsymbol{R}') c_{j\sigma'}(\boldsymbol{R}') c_{i\sigma}(\boldsymbol{R}),$$
(1)

where $\boldsymbol{R}$ are the coordinates of the Bravais lattice, $i$, $j$ are the labels of the sublattice/layer, $c_{i\sigma}(\boldsymbol{R})$ is the the quantum operator for the annihilation of one electron with spin $\sigma$ in the $p_z$ orbital localized at the position $\boldsymbol{R} + \delta_i$, $\delta_i$ being the internal coordinate in the unit cell, and

$$V_C^{ij}(\boldsymbol{R}-\boldsymbol{R}') = \frac{e^2}{4\pi\epsilon|\boldsymbol{R}-\boldsymbol{R}'+\delta_i-\delta_j|}$$
(2)

is the Coulomb potential, where $e$ is the electron charge and $\epsilon$ is the dielectric constant of the environment, $\epsilon = \epsilon_0$ in the vacuum. Next, we consider the continuum limit of the lattice model, by expanding the operators $c$ as

$$c_{i\sigma}(\boldsymbol{R}) \equiv A_c^{1/2}\big[\psi_{i\sigma}^K(\boldsymbol{R})e^{iK\cdot\boldsymbol{R}} + \psi_{i\sigma}^{K'}(\boldsymbol{R})e^{iK'\cdot\boldsymbol{R}}\big],$$
(3)

where $A_c = \sqrt{3}a^2/2$ is the area of the unit cell of graphene, $a = 2.46$ Å being the lattice constant, $K$, $K'$ are the nonequivalent corners of the Brillouin zone (BZ), and $\psi_{i\sigma}^K(\boldsymbol{r})$, $\psi_{i\sigma}^{K'}(\boldsymbol{r})$ are fermionic operators, which vary smoothly with the continuum position $\boldsymbol{r}$ and represent the valley projections of $c_{i\sigma}(\boldsymbol{R})$. Replacing Eq. (3) into Eq. (1), among all the terms one finds the following valley-exchange interaction,

$$\hat{H}_{\text{exc}} = A_c^2 \sum_{\boldsymbol{R}\boldsymbol{R}'} \sum_{ij\sigma\sigma'} \psi_{i\sigma}^{K,\dagger}(\boldsymbol{R}) \psi_{j\sigma'}^{K',\dagger}(\boldsymbol{R}') \psi_{j\sigma'}^K(\boldsymbol{R}') \psi_{i\sigma}^{K'}(\boldsymbol{R}) V_C^{ij}$$

$$\times (\boldsymbol{R}-\boldsymbol{R}') e^{-i\Delta K\cdot(\boldsymbol{R}-\boldsymbol{R}')},$$
(4)

which describes the intervalley scattering processes. As we show in detail in the SM [53], Eq. (4) can be safely approximated by the continuum Hamiltonian,

$$\hat{H}_{\text{exc}} \simeq -J \sum_{i\sigma\sigma'} \int d^2\boldsymbol{r}\, \psi_{i\sigma}^{K,\dagger}(\boldsymbol{r}) \psi_{i\sigma'}^{K',\dagger}(\boldsymbol{r}) \psi_{i\sigma}^{K'}(\boldsymbol{r}) \psi_{i\sigma'}^K(\boldsymbol{r}),$$
(5)

where $J \equiv \frac{e^2}{2\epsilon|\Delta K|}$ is the Fourier transform of the Coulomb potential in two dimensions (2D), evaluated at $\Delta K$. It is worth noting that the interaction described by Eq. (5) is purely local, not only in the space coordinates, but also in the sublattice and layer indices. Because $J > 0$, $\hat{H}_{\text{exc}}$ provides an effective attraction in the spin-triplet channel (see SM [53]), favoring the Cooper pairing with electrons in opposite valleys. This kind of interaction belongs to the universality class identified by Crepel and Fu [54,55], who have demonstrated the relevance of the valley-exchange interaction in inducing the pairing in narrow-band systems. As we already mentioned, we stress that the spin-triplet superconductivity is a general claim of the experimental works. On the other hand, the valley exchange from the Coulomb interaction has been shown to favor spin-triplet superconductivity in various materials (see, for example, Refs. [29,56,57]). The SC OP, $\Delta^i(\boldsymbol{r})$, is purely local and the value of $T_c$ can be obtained within the BCS theory as the largest temperature for which there exists a

nonzero solution of the linearized gap equation,

$$\Delta^i(\boldsymbol{r}) = \frac{J}{\beta} \sum_j \int d\boldsymbol{r}' \sum_{l=-\infty}^{+\infty}$$

$$\times \mathcal{G}_{ij}^K(\boldsymbol{r}, \boldsymbol{r}'; i\omega_l) \mathcal{G}_{ij}^{K'}(\boldsymbol{r}, \boldsymbol{r}'; -i\omega_l) \Delta^j(\boldsymbol{r}'),$$
(6)

where $\beta = (K_B T)^{-1}$ is the inverse of the temperature, $\omega_l = \pi(2l+1)/(\hbar\beta)$ are fermionic Matsubara frequencies, and $\mathcal{G}^{K,K'}$ are the Green's function for the $K$, $K'$ valleys, respectively, computed in the normal phase. Equation (6) is written in real space in order to be as general as possible, holding also for nontranslationally invariant systems, as is the case of the TBG that we will consider below.

It is worth noting that (i) $J$ is generally small. For example, if we consider $\epsilon/\epsilon_0 = 4$, which mimics the screening by a substrate of hexagonal boron nitride (hBN), then $J \simeq 13.25$ eV Å$^2$, consistent with the estimates of the Hubbard interaction strength in graphene [58–62]. Such a small value requires a large DOS at the Fermi energy $N_F$ to make the dimensionless SC coupling, $\lambda = N_F J$, sizable. While the DOS is suppressed in the monolayer graphene close to charge neutrality, multilayer stacks of graphene offer a way to increase the value of $N_F$, and hence to strengthen $\lambda$, upon tuning a number of experimental parameters, such as, e.g., the relative twist between the layers, the electronic density, the displacement field etc. (ii) We are not considering the effects of the intravalley scattering induced by the Coulomb interaction at small momenta, which are repulsive. In a van Hove scenario, these terms are suppressed by the strong internal screening. As we show in the SM [53] for the case of the RTG, the strength of the screened intravalley Coulomb repulsion is orders of magnitude smaller than $J$, which fully justifies its omission. (iii) We are not considering the internal screening of $J$, which is supposed to be negligible as it is induced by the particle-hole excitations with the particle and the hole in opposite valleys. These kinds of processes are indeed suppressed despite a large DOS. This assumption is justified quantitatively in the SM [53], where we show that the screening essentially does not affect the value of $J$ as compared to its bare value.

## III. RESULTS

*The case of the TBG.* A relatively small twist $\theta$ between the two layers of a bilayer graphene generates a moiré superlattice with periodicity $L_m \simeq a/\theta$, much larger than the lattice constant of the monolayer graphene. The interlayer hopping varies smoothly at the scale of the moiré, breaking the translational invariance within each moiré unit cell and strongly hybridizing the $p_z$ orbitals of the constitutive graphene sheets. The superconductivity has been observed at the "magic" angle, $\theta = 1.05°$ [1–3], where the free-electron spectrum features two weakly dispersing narrow bands at the charge neutrality point (CNP), generating strong VHSs in the DOS [63,64].

Using the continuum model of the TBG [63–66], we solve the linearized gap equation (6) as detailed in the SM [53]. Figure 1 shows $T_c$ as a function of the filling per moiré unit cell $\nu$ obtained for three values of the twist angle, as coded in the caption, and for $\epsilon/\epsilon_0 = 4$. We find values of $T_c$ of the order

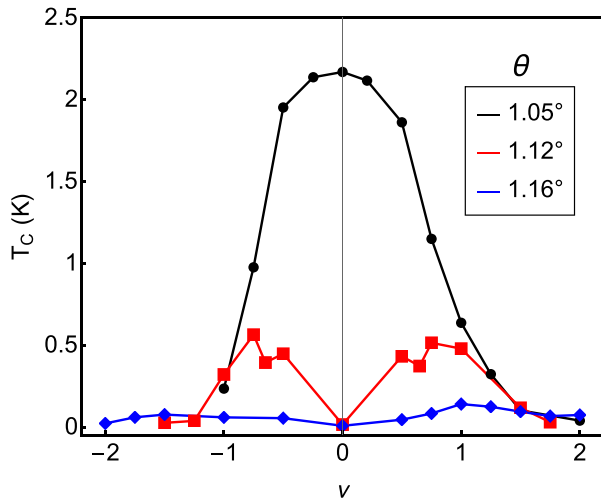FIG. 1. $T_c$ as a function of the filling, obtained for $\epsilon/\epsilon_0 = 4$ and $\theta = 1.05°, 1.12°, 1.16°$.



FIG. 3. $T_c$ of the (a) hole-doped RTG and (b) BBG as a function of $n_e$, obtained for $\epsilon/\epsilon_0 = 4$ and $\Delta_1$ as coded in the inset panel.

of 1 K, in good agreement with the experimental findings. $T_c$ is the largest for $\theta = 1.05°$, where the bandwidth at the CNP is minimum. The band structure and the DOS corresponding to the two central bands of the TBG at $\theta = 1.05°$ are shown in Fig. 2 for $\nu = -1, 0, 1$. The continuous and the dashed lines refer to the $K$ and $K'$ valleys, respectively, while the horizontal lines identify the Fermi energies. Note that the reshaping of the bands with the filling is induced by the Hartree corrections [8,10]. Comparing Figs. 1 and 2 makes it clear that the value of $T_c$ increases with $N_F$, which explains why we obtain the largest $T_c$ at $\nu = 0$, where the bandwidth is minimum. It is worth noting that the TBG is actually a flavor polarized insulator at $\nu = 0$. As we are not considering flavor polarized phases, the superconductivity that we obtain at $\nu = 0$ is not realistic. Nonetheless, it serves as an example to grab the relevance of the VHSs in inducing the pairing. As we show in the SM [53], the order of magnitude of $T_c$ and its $\nu$
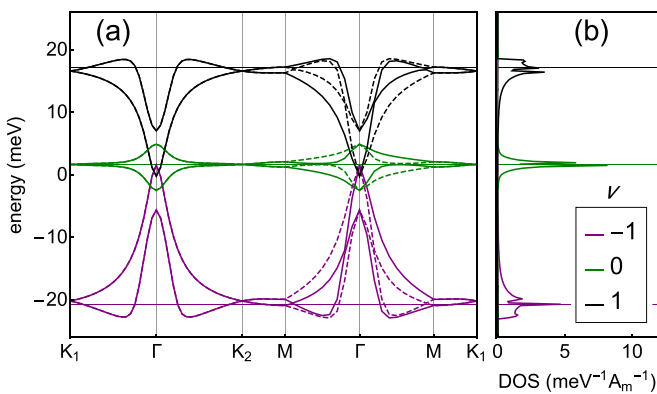
dependence do not change for realistic values of the external screening, $\epsilon/\epsilon_0 \sim 4$–6.

The OP, $\Delta^i(\boldsymbol{r})$, that we obtain as a solution of Eq. (6) at $T = T_c$, is almost uniform in the sublattices and layers, has a constant phase and varies in the moiré unit cell, reaching its maxima in the regions with local $AA$ stacking. Maps of $\Delta^i(\boldsymbol{r})$ are shown in the SM [53].

*The case of the RTG and BBG.* Both RTG and BBG become superconductors at very low electronic densities, $n_e \sim 10^{12}$ cm$^{-2}$, when an electric field is applied perpendicular to the graphene's flakes [5,6]. The experimental $T_c$'s are $\sim 10^{-1}$ K for the RTG and $\sim 10^{-2}$ K for the BBG. From an electronic point of view, a perpendicular electric field breaks the inversion symmetry and gaps out the Dirac points in both RTG and BBG. The nearly flat dispersion close to the gap's edge gives rise to a pronounced VHS. For values of $n_e$ close to those at which the superconductivity has been reported, the Fermi level lies near the VHS.

We study the low-energy continuum model of the RTG and BBG, with the hopping amplitudes given by Refs. [28,67,68], and an interlayer bias $\Delta_1$ describing the perpendicular electric field (see SM [53]). We extract $T_c$ by using the linearized gap equation (6) in the translationally invariant case, as detailed in the SM [53]. Figure 3 shows the values of $T_c$ as a function of $n_e$ in the hole-doped RTG [Fig. 3(a)] and BBG [Fig. 3(b)], obtained for $\epsilon/\epsilon_0 = 4$ and realistic values of $\Delta_1$, as coded in the inset panel. We obtain critical temperatures up to $\sim 130$–140 mK for the RTG, and up to $\sim 20$ mK for the BBG, approximately one order of magnitude smaller than in RTG. The peak's intensity and position depend on $\Delta_1$. These estimates of $T_c$ are in excellent agreement with the two experiments [5,6]. Reference [5] identifies two distinct SC phases of the RTG, named SC1 and SC2. While the former does respect the Pauli limit, the latter does not, implying that the pairing is spin unpolarized in SC1 and spin polarized in SC2. The superconductivity observed in the BBG in Ref. [6] is always accompanied by the violation of the Pauli limit, suggesting that the SC1 phase is absent in the BBG. It is worth noting that the spin-triplet pairing that we are considering is compatible with both spin-unpolarized and spin-polarized Cooper pairs, and consequently it does not exclude *a priori* either the SC1 or the SC2 regime. However, comparing the values of $T_c$



FIG. 2. (a) Band structure and (b) DOS corresponding to the two central bands of the TBG, obtained for $\theta = 1.05°$ and $\nu = -1, 0, 1$. The continuous and the dashed lines refer to the $K$ and $K'$ valleys, respectively, while the horizontal lines identify the Fermi energies. The DOS is expressed in units of meV$^{-1} A_m^{-1}$, where $A_m = \sqrt{3}L_m^2/2$ is the area of the moiré unit cell.

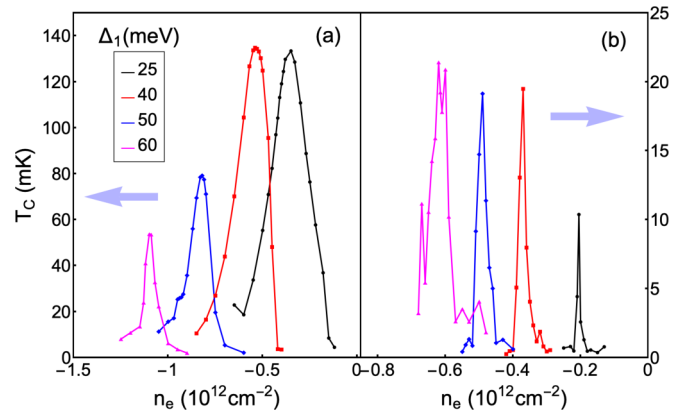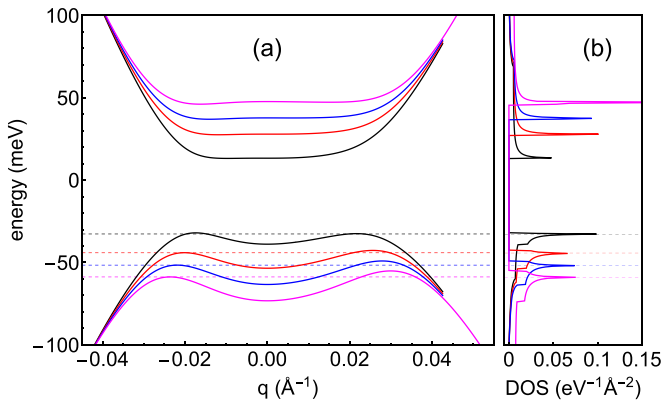FIG. 4. (a) Band structure and (b) DOS of the RTG close to the CNP, obtained for $\Delta_1 = 25$, 40, 50, and 60 meV, and color coded as in Fig. 3. Here, $q = 0$ at the $K$ point. The horizontal dashed lines indicate the Fermi levels corresponding to the densities that maximize $T_c$ in Fig. 3.

in Fig. 3(a) with the experimental temperatures reported in Ref. [5], it seems that our calculations are missing the SC2 phase of the RTG. Remarkably, our results reproduce quite well both the range of $n_e$ in which the superconductivity has been reported and the narrowness of the SC domain. Figure 4 shows the band structure [Fig. 4(a)] and DOS [Fig. 4(b)] of the RTG close to the CNP, obtained for the values of $\Delta_1$ considered in Fig. 3 and color coded as there. The bands flatten close to the gap edge, giving rise to the VHSs in the DOS, whose position and intensity can be tuned by $\Delta_1$. The horizontal dashed lines indicate the Fermi levels corresponding to the densities that maximize $T_c$ in Fig. 3, emphasizing that the superconductivity is strongly favored when the Fermi level matches the VHS. The spectral feature of the BBG in the presence of a perpendicular electric field is qualitatively very similar to that of the RTG. The narrowness of the SC domain can be explained by considering that the bands of the

RTG and BBG remain rigid upon tuning $n_e$, that only moves the Fermi level. Thus, there is only a small range of values of $n_e$ for which the Fermi level lies near the VHS. This is in stark contrast to the case of the TBG, where the shape of the bands changes with the filling in order to pin the VHS to the Fermi level [8,10], then allowing for wide SC domains.

Finally, we find that the SC OP is fully localized in the layer and sublattice in which the electric field confines the low-energy electrons, as shown in Ref. [69].

## IV. CONCLUSIONS

Our work represents one step further in the study of the origin of the superconductivity recently observed in a few layers of graphene, that can be explained by a universal purely electronic mechanism, in which the valley exchange induced by the Coulomb repulsion serves as the pairing glue in the valley-singlet/spin-triplet Cooper channel. The pairing is then favored by the proximity of the Fermi level to the VHSs, that can be achieved in these materials by tuning a set of experimental parameters. Exploiting low-energy continuum models, we provide a general method for computing the SC critical temperature as well as the symmetry of the OP, and we test it in three representative systems, TBG, RTG, and BBG, obtaining excellent agreement with the experimental findings. Beyond the case of graphene-based heterostructures, our analysis might be generalized to study the pairing in a wider class of materials displaying valley degrees of freedom and VHSs, as is the case of the recently discovered superconductors on silicon surfaces [70–72].

[1] Y. Cao, V. Fatemi, S. Fang, K. Watanabe, T. Taniguchi, E. Kaxiras, and P. Jarillo-Herrero, Unconventional superconductivity in magic-angle graphene superlattices, Nature (London) **556**, 43 (2018).

[2] X. Lu, P. Stepanov, W. Yang, M. Xie, M. A. Aamir, I. Das, C. Urgell, K. Watanabe, T. Taniguchi, G. Zhang, A. Bachtold, A. H. MacDonald, and D. K. Efetov, Superconductors, orbital magnets and correlated states in magic-angle bilayer graphene, Nature (London) **574**, 653 (2019).

[3] M. Yankowitz, S. Chen, H. Polshyn, Y. Zhang, K. Watanabe, T. Taniguchi, D. Graf, A. F. Young, and C. R. Dean, Tuning superconductivity in twisted bilayer graphene, Science **363**, 1059 (2019).

[4] J. M. Park, Y. Cao, K. Watanabe, T. Taniguchi, and P. Jarillo-Herrero, Tunable strongly coupled superconductivity in magic-angle twisted trilayer graphene, Nature (London) **590**, 249 (2021).

[5] H. Zhou, T. Xie, T. Taniguchi, K. Watanabe, and A. F. Young, Superconductivity in rhombohedral trilayer graphene, Nature (London) **598**, 434 (2021).

[6] H. Zhou, L. Holleis, Y. Saito, L. Cohen, W. Huynh, C. L. Patterson, F. Yang, T. Taniguchi, K. Watanabe, and A. F. Young, Isospin magnetism and spin-polarized superconductivity in Bernal bilayer graphene, Science **375**, 774 (2022).

[7] Y. Zhang, R. Polski, A. Thomson, É. Lantagne-Hurtubise, C. Lewandowski, H. Zhou, K. Watanabe, T. Taniguchi, J. Alicea, and S. Nadj-Perge, Spin-orbit enhanced superconductivity in Bernal bilayer graphene, arXiv:2205.05087.

[8] F. Guinea and N. R. Walet, Electrostatic effects, band distortions, and superconductivity in twisted graphene bilayers, Proc. Natl. Acad. Sci. USA **115**, 13174 (2018).

[9] Y. Sherkunov and J. J. Betouras, Electronic phases in twisted bilayer graphene at magic angles as a result of van Hove singularities and interactions, Phys. Rev. B **98**, 205151 (2018).

[10] T. Cea, N. R. Walet, and F. Guinea, Electronic band structure and pinning of Fermi energy to van Hove singularities in twisted bilayer graphene: A self-consistent approach, Phys. Rev. B **100**, 205113 (2019).

[11] T. Cea and F. Guinea, Band structure and insulating states driven by Coulomb interaction in twisted bilayer graphene, Phys. Rev. B **102**, 045107 (2020).

[12] Y.-P. Lin and R. M. Nandkishore, Parquet renormalization group analysis of weak-coupling instabilities with multiple high-order van Hove points inside the Brillouin zone, Phys. Rev. B **102**, 245122 (2020).

[13] D. V. Chichinadze, L. Classen, Y. Wang, and A. V. Chubukov, Cascade of transitions in twisted and non-twisted graphene layers within the van Hove scenario, npj Quantum Mater. **7**, 114 (2022).

[14] H. Isobe, N. F. Q. Yuan, and L. Fu, Unconventional Superconductivity and Density Waves in Twisted Bilayer Graphene, Phys. Rev. X **8**, 041041 (2018).

[15] C.-C. Liu, L.-D. Zhang, W.-Q. Chen, and F. Yang, Chiral Spin Density Wave and $d + id$ Superconductivity in the Magic-Angle-Twisted Bilayer Graphene, Phys. Rev. Lett. **121**, 217001 (2018).

[16] J. González and T. Stauber, Kohn-Luttinger Superconductivity in Twisted Bilayer Graphene, Phys. Rev. Lett. **122**, 026801 (2019).

[17] Y.-Z. You and A. Vishwanath, Superconductivity from valley fluctuations and approximate SO(4) symmetry in a weak coupling theory of twisted bilayer graphene, npj Quantum Mater. **4**, 16 (2019).

[18] B. Roy and V. Juričić, Unconventional superconductivity in nearly flat bands in twisted bilayer graphene, Phys. Rev. B **99**, 121407(R) (2019).

[19] G. Sharma, M. Trushin, O. P. Sushkov, G. Vignale, and S. Adam, Superconductivity from collective excitations in magic-angle twisted bilayer graphene, Phys. Rev. Res. **2**, 022040(R) (2020).

[20] D. V. Chichinadze, L. Classen, and A. V. Chubukov, Nematic superconductivity in twisted bilayer graphene, Phys. Rev. B **101**, 224513 (2020).

[21] W. Qin, B. Zou, and A. H. MacDonald, Critical magnetic fields and electron-pairing in magic-angle twisted bilayer graphene, arXiv:2102.10504.

[22] Z. Dong and L. Levitov, Activating superconductivity in a repulsive system by high-energy degrees of freedom, arXiv:2103.08767.

[23] A. Ghazaryan, T. Holder, M. Serbyn, and E. Berg, Unconventional Superconductivity in Systems with Annular Fermi Surfaces: Application to Rhombohedral Trilayer Graphene, Phys. Rev. Lett. **127**, 247001 (2021).

[24] H. Dai, J. Hou, X. Zhang, Y. Liang, and T. Ma, Mott insulating state and $d + id$ superconductivity in an ABC graphene trilayer, Phys. Rev. B **104**, 035104 (2021).

[25] J. Gonzalez and T. Stauber, Ising superconductivity induced from valley symmetry breaking in twisted trilayer graphene, arXiv:2110.11294.

[26] A. Fischer, Z. A. H. Goodwin, A. A. Mostofi, J. Lischner, D. M. Kennes, and L. Klebl, Unconventional superconductivity in magic-angle twisted trilayer graphene, npj Quantum Mater. **7**, 5 (2022).

[27] A. L. Szabó and B. Roy, Metals, fractional metals, and superconductivity in rhombohedral trilayer graphene, Phys. Rev. B **105**, L081407 (2022).

[28] T. Cea, P. A. Pantaleón, V. T. Phong, and F. Guinea, Superconductivity from repulsive interactions in rhombohedral trilayer graphene: A Kohn-Luttinger-like mechanism, Phys. Rev. B **105**, 075432 (2022).

[29] W. Qin, C. Huang, T. Wolf, N. Wei, I. Blinov, and A. H. MacDonald, Functional renormalization group study of superconductivity in rhombohedral trilayer graphene, arXiv:2203.09083.

[30] V. Crépel, T. Cea, L. Fu, and F. Guinea, Unconventional superconductivity due to interband polarization, Phys. Rev. B **105**, 094506 (2022).

[31] D.-C. Lu, T. Wang, S. Chatterjee, and Y.-Z. You, Correlated metals and unconventional superconductivity in rhombohedral trilayer graphene: A renormalization group analysis, Phys. Rev. B **106**, 155115 (2022).

[32] A. Jimeno-Pozo, H. Sainz-Cruz, T. Cea, P. A. Pantaleón, and F. Guinea, Superconductivity from electronic interactions and spin-orbit enhancement in bilayer and trilayer graphene, arXiv:2210.02915.

[33] F. Wu, A. H. MacDonald, and I. Martin, Theory of Phonon-Mediated Superconductivity in Twisted Bilayer Graphene, Phys. Rev. Lett. **121**, 257001 (2018).

[34] T. J. Peltonen, R. Ojajärvi, and T. T. Heikkilä, Mean-field theory for superconductivity in twisted bilayer graphene, Phys. Rev. B **98**, 220504(R) (2018).

[35] Y. W. Choi and H. J. Choi, Strong electron-phonon coupling, electron-hole asymmetry, and nonadiabaticity in magic-angle twisted bilayer graphene, Phys. Rev. B **98**, 241412(R) (2018).

[36] B. Lian, Z. Wang, and B. A. Bernevig, Twisted Bilayer Graphene: A Phonon-Driven Superconductor, Phys. Rev. Lett. **122**, 257002 (2019).

[37] M. Angeli, E. Tosatti, and M. Fabrizio, Valley Jahn-Teller Effect in Twisted Bilayer Graphene, Phys. Rev. X **9**, 041010 (2019).

[38] F. Wu, E. Hwang, and S. Das Sarma, Phonon-induced giant linear-in-$T$ resistivity in magic angle twisted bilayer graphene: Ordinary strangeness and exotic superconductivity, Phys. Rev. B **99**, 165112 (2019).

[39] F. Schrodi, A. Aperis, and P. M. Oppeneer, Prominent Cooper pairing away from the Fermi level and its spectroscopic signature in twisted bilayer graphene, Phys. Rev. Res. **2**, 012066(R) (2020).

[40] Y. W. Choi and H. J. Choi, Dichotomy of Electron-Phonon Coupling in Graphene Moiré Flat Bands, Phys. Rev. Lett. **127**, 167001 (2021).

[41] Y.-Z. Chou, F. Wu, J. D. Sau, and S. Das Sarma, Acoustic-Phonon-Mediated Superconductivity in Rhombohedral Trilayer Graphene, Phys. Rev. Lett. **127**, 187001 (2021).

[42] Y.-Z. Chou, F. Wu, J. D. Sau, and S. Das Sarma, Acoustic-phonon-mediated superconductivity in Bernal bilayer graphene, Phys. Rev. B **105**, L100503 (2022).

[43] S. Firoz Islam, A. Y. Zyuzin, and A. A. Zyuzin, Unconventional superconductivity with preformed pairs in twisted bilayer graphene, arXiv:2208.12039.

[44] C. Lewandowski, D. Chowdhury, and J. Ruhman, Pairing in magic-angle twisted bilayer graphene: Role of phonon and plasmon umklapp, Phys. Rev. B **103**, 235401 (2021).

[45] C. Lewandowski, S. Nadj-Perge, and D. Chowdhury, Does filling-dependent band renormalization aid pairing in twisted bilayer graphene? npj Quantum Mater. **6**, 82 (2021).

[46] T. Cea and F. Guinea, Coulomb interaction, phonons, and superconductivity in twisted bilayer graphene, Proc. Natl. Acad. Sci. USA **118**, e2107874118 (2021).

[47] V. T. Phong, P. A. Pantaleón, T. Cea, and F. Guinea, Band structure and superconductivity in twisted trilayer graphene, Phys. Rev. B **104**, L121116 (2021).

[48] H. C. Po, L. Zou, A. Vishwanath, and T. Senthil, Origin of Mott Insulating Behavior and Superconductivity in Twisted Bilayer Graphene, Phys. Rev. X **8**, 031089 (2018).

[49] V. Kozii, M. P. Zaletel, and N. Bultinck, Spin-triplet superconductivity from intervalley Goldstone modes in magic-angle graphene, Phys. Rev. B **106**, 235157 (2022).

[50] S. Chatterjee, T. Wang, E. Berg, and M. P. Zaletel, Inter-valley coherent order and isospin fluctuation mediated superconductivity in rhombohedral trilayer graphene, Nat. Commun. **13**, 6013 (2022).

[51] Z. Dong and L. Levitov, Superconductivity in the vicinity of an isospin-polarized state in a cubic Dirac band, arXiv:2109.01133.

[52] Z. Dong, A. V. Chubukov, and L. Levitov, Spin-triplet superconductivity at the onset of isospin order in biased bilayer graphene, arXiv:2205.13353.

[53] See Supplemental Material at http://link.aps.org/supplemental/10.1103/PhysRevB.107.L041111 for the intervalley scattering from the Coulomb repulsion and the induced Cooper pairing, the case of the TBG, the case of the RTG and BBG, and screening of the Coulomb interaction.

[54] V. Crépel and L. Fu, New mechanism and exact theory of superconductivity from strong repulsive interaction, Sci. Adv. **7**, eabh2233 (2021).

[55] V. Crépel and L. Fu, Spin-triplet superconductivity from excitonic effect in doped insulators, Proc. Natl. Acad. Sci. USA **119**, e2117735119 (2022).

[56] F. Guinea and B. Uchoa, Odd-momentum pairing and superconductivity in vertical graphene heterostructures, Phys. Rev. B **86**, 134521 (2012).

[57] R. Roldán, E. Cappelluti, and F. Guinea, Interactions and superconductivity in heavily doped $MoS_2$, Phys. Rev. B **88**, 054515 (2013).

[58] R. G. Parr, D. P. Craig, and I. G. Ross, Molecular orbital calculations of the lower excited electronic levels of benzene, configuration interaction included, J. Chem. Phys. **18**, 1561 (1950).

[59] K. Ohno, Some remarks on the Pariser-Parr-Pople method, Theor. Chim. Acta **2**, 219 (1964).

[60] N. C. Baird and M. J. S. Dewar, Ground states of $\sigma$-bonded molecules. IV. The Mindo method and its application to hydrocarbons, J. Chem. Phys. **50**, 1262 (1969).

[61] J. A. Vergés, E. SanFabián, G. Chiappe, and E. Louis, Fit of Pariser-Parr-Pople and Hubbard model Hamiltonians to charge and spin states of polycyclic aromatic hydrocarbons, Phys. Rev. B **81**, 085120 (2010).

[62] T. O. Wehling, E. Şaşıoğlu, C. Friedrich, A. I. Lichtenstein, M. I. Katsnelson, and S. Blügel, Strength of Effective Coulomb Interactions in Graphene and Graphite, Phys. Rev. Lett. **106**, 236805 (2011).

[63] J. M. B. Lopes dos Santos, N. M. R. Peres, and A. H. Castro Neto, Graphene Bilayer with a Twist: Electronic Structure, Phys. Rev. Lett. **99**, 256802 (2007).

[64] R. Bistritzer and A. H. MacDonald, Moiré bands in twisted double-layer graphene, Proc. Natl. Acad. Sci. USA **108**, 12233 (2011).

[65] J. M. B. Lopes dos Santos, N. M. R. Peres, and A. H. Castro Neto, Continuum model of the twisted graphene bilayer, Phys. Rev. B **86**, 155449 (2012).

[66] M. Koshino, N. F. Q. Yuan, T. Koretsune, M. Ochi, K. Kuroki, and L. Fu, Maximally Localized Wannier Orbitals and the Extended Hubbard Model for Twisted Bilayer Graphene, Phys. Rev. X **8**, 031087 (2018).

[67] A. A. Zibrov, P. Rao, C. Kometter, E. M. Spanton, J. I. A. Li, C. R. Dean, T. Taniguchi, K. Watanabe, M. Serbyn, and A. F. Young, Emergent Dirac Gullies and Gully-Symmetry-Breaking Quantum Hall States in *ABA* Trilayer Graphene, Phys. Rev. Lett. **121**, 167601 (2018).

[68] H. Zhou, T. Xie, A. Ghazaryan, T. Holder, J. R. Ehrets, E. M. Spanton, T. Taniguchi, K. Watanabe, E. Berg, M. Serbyn, and A. F. Young, Half- and quarter-metals in rhombohedral trilayer graphene, Nature (London) **598**, 429 (2021).

[69] F. Zhang, B. Sahu, H. Min, and A. H. MacDonald, Band structure of *ABC*-stacked graphene trilayers, Phys. Rev. B **82**, 035409 (2010).

[70] T. Nakamura, H. Kim, S. Ichinokura, A. Takayama, A. V. Zotov, A. A. Saranin, Y. Hasegawa, and S. Hasegawa, Unconventional superconductivity in the single-atom-layer alloy Si(111)-$\sqrt{3}\times\sqrt{3}$-(Tl, Pb), Phys. Rev. B **98**, 134505 (2018).

[71] X. Wu, F. Ming, T. S. Smith, G. Liu, F. Ye, K. Wang, S. Johnston, and H. H. Weitering, Superconductivity in a Hole-Doped Mott-Insulating Triangular Adatom Layer on a Silicon Surface, Phys. Rev. Lett. **125**, 117001 (2020).

[72] F. Ming, X. Wu, C. Chen, K. D. Wang, P. Mai, T. A. Maier, J. Strockoz, J. W. F. Venderbos, C. Gonzalez, J. Ortega, S. Johnston, and H. H. Weitering, Evidence for chiral superconductivity on a silicon surface, arXiv:2210.06273.